

# Arterial Wave Separation Analysis and Reflection Wave Transit Time Estimation using a Double Rayleigh Flow Rate Model

Rahul Manoj, Aneesh S, Raj Kiran V, Nabeel P M, *Member IEEE*, Mohanasankar Sivaprakasam and Jayaraj Joseph

**Abstract**— Arterial pulse wave separation analysis (WSA) requires simultaneously measured pressure and flow rate waveform from the same arterial site. Modelling approaches to flow rate waveforms offers a methodological and instrumental advantage. However, current techniques are limited to the aortic site. For non-aortic sites such as carotid artery, modelling methods that were developed for aortic sites are not likely to capture the intrinsic differences in the carotid flow rate. In this work, a double-Rayleigh flow rate model for the carotid artery is developed to separate the forward and backward pressure waves using WSA (DRM<sub>WSA</sub>). The model parameters are optimally found based on characteristic features - obtained from the pressure waveform. The DRM<sub>WSA</sub> was validated using a database of 4374 virtual (healthy) subjects, and its performance was compared with actual flow rate based WSA (REF<sub>WSA</sub>) at the carotid artery. An RMSE < 2 mmHg were obtained for forward and backward pressure waveforms. The reflection quantification indices ( $\Delta P_F$ ,  $\Delta P_B$ ), (RM, RI) obtained from DRM<sub>WSA</sub> demonstrated strong and statistically significant correlation ( $r > 0.96$ ,  $p < 0.001$ ) and ( $r > 0.80$ ,  $p < 0.001$ ) respectively, with insignificant bias ( $p > 0.05$ ), upon comparing with counterparts in REF<sub>WSA</sub>. A moderate correlation ( $r = 0.64$ ,  $p < 0.001$ ) was obtained for reflection wave transit time between both methods. The proposed method minimises the measurements required for WSA and has the potential to widen the vascular screening procedures incorporating carotid pulse wave dynamics.

**Clinical Relevance**—This methodology quantifies arterial pressure wave reflections in terms of pressure augmentation and reflection transit time. The methodological advantage of using only a single waveform helps easy translation to technological solutions for clinical research.

## I. INTRODUCTION

The left ventricle acts as a pulsatile pump and ejects a blood volume into the arterial system. The impulse generated by the left ventricle propagates at a finite speed from proximal

\*This research was partially supported by Science and Engineering Research Board (SERB), Department of Science and Technology (DST) and Indian Institute of Technology (IIT) Madras under Institute of Eminence (IoE) funding from the Ministry of Human Resource Development (MHRD), Government of India.

Rahul Manoj and Raj Kiran V are with the Department of Electrical Engineering, Indian Institute of Technology Madras (IIT M), Chennai-600036, Tamil Nadu, India (e-mail: rahulmanojktym@gmail.com).

Aneesh S is with the Department of Electrical and Electronics Engineering, National Institute of Technology Tiruchirappalli (NIT T), Tamil Nadu-620015, India

Nabeel P M is with Healthcare Technology Innovation Centre (HTIC), Indian Institute of Technology Madras Research Park, Chennai-600113, Tamil Nadu, India.

Jayaraj Joseph and Mohanasankar Sivaprakasam is with the faculty of Electrical Engineering at Indian Institute of Technology Madras (IIT M), Chennai-600036, Tamil Nadu, India.

to distal arteries as a forward-running wave. However, this wave is not perfectly absorbed by the arterial system and results in various degrees of reflections as multiple backward-running waves returning to the left ventricle [1]. The source of reflections in vasculature is the mismatch of impedance as seen by the forward wave. They are due in part to the changes in structural properties (tapering of diameters, branching of vessels) and material properties (stiffness and stiffness gradient) from central to peripheral arteries. The reflection of pressure waves causes pressure augmentation (widening the pulse pressure), altering the hemostasis at the microcirculation and leads to end-organ damage [2]. On the other hand, early onset of backward waves during the systolic phase increases cardiac afterload [3] and reduces the ventricular pump efficiency [4]. Thus, the quantification of the pressure augmentation and transit time between forward and backward waves is of increasing interest in the research and clinical community.

Among the methods developed in quantifying the reflections, augmentation index (AIx) received wider attention in clinical research [5]. However, several factors such as the height of the individual, accurate identification of shoulder point, compounding effect of heart rate and arterial stiffness gradient challenges the reliability of AIx and has a debatable role in quantifying reflections [6]. A more reliable method to quantify reflections is Wave Separation Analysis (WSA). Accurate WSA requires simultaneously measured arterial pressure and blood flow rate waveform (ideally from a single arterial site). The implementation of WSA is carried out in the frequency domain as impedance analysis [7] or in the time domain from successive wavefront analysis [8]. Simultaneous and synchronised acquisition of pressure and flow rate waveform from the same arterial site (aortic) imposes a practical challenge. Subsequently, simplified approaches to WSA have been proposed, based on approximations to flow rate waveform [9]–[11]. The applicability and validation of simplified WSA were limited to aortic flow rate waveforms in the literature.

In this article, we propose a double Rayleigh model (DRM) to approximate the carotid flow rate waveform. The WSA performed at the carotid artery is of interest due to its association with central arteries, closely representing aortic conditions and for its practical advantages in easier accessibility for non-invasive measurements. The proposed method is validated against the actual flow-based WSA and its performance is evaluated in terms of the reflection quantification indices (refer to Fig.1).

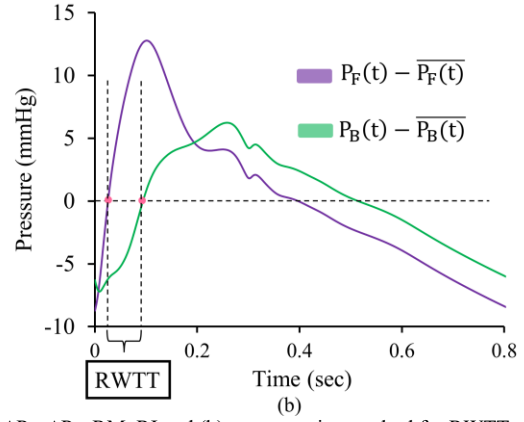
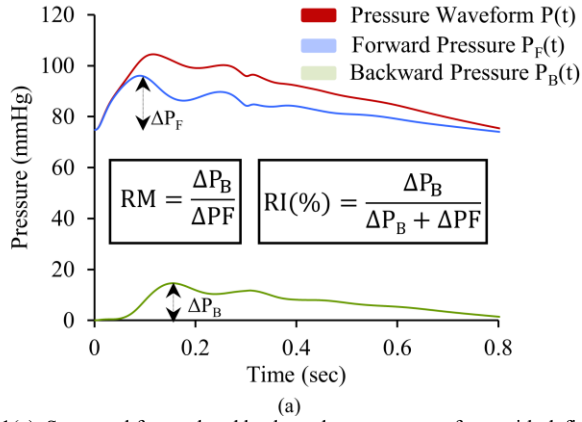


Fig.1(a). Separated forward and backward pressure waveform with definitions of  $\Delta P_F$ ,  $\Delta P_B$ , RM, RI and (b) zero-crossing method for RWTT

## II. METHODS

### A. Double Rayleigh Flow Rate Model & Wave Separation

The WSA combines the transmission line circuit analogy with water hammer relationships [7] to obtain expressions for forward ( $P_F(t)$ ) and backward pressure waveform ( $P_B(t)$ ) as,

$$P_F(t) = \frac{1}{2} (P(t) + Q(t) \times Z_C) \quad (1)$$

and

$$P_B(t) = \frac{1}{2} (P(t) - Q(t) \times Z_C) \quad (2)$$

where  $P(t)$  is the transmural pressure waveform,  $Q(t)$  is the corresponding flow rate waveform either measured or modelled and  $Z_C$  is the magnitude of the characteristic impedance of the arterial blood vessel under consideration.

The flow rate during the ejection period of the heart is modelled as a double-Rayleigh function ( $Q_{DRM}(t)$ ) with model parameters ( $\sigma_1$ ,  $\sigma_2$ ).

$$Q_{DRM}(t) = \frac{t}{\sigma_1^2} \times e^{-t^2/2\sigma_1^2} + \frac{t}{\sigma_2^2} \times e^{-t^2/2\sigma_2^2} \quad (3)$$

The model parameters ( $\sigma_1$ ,  $\sigma_2$ ) are optimally found iteratively such that the absolute error functions ( $F_1$  and  $F_2$ ) are minimized at the time instant of peak flow rate ( $\tau_{peak}$ ) and ejection period ( $\tau_{EP}$ ) of actual carotid flow rate waveform  $Q_{REF}(t)$  as in (4) and (5).

$$F_1 = |\tau_{peak}(Q_{DRM}(t)) - \tau_{peak}(Q_{REF}(t))| \quad (4)$$

$$F_2 = |\tau_{base}(Q_{DRM}(t)) - \tau_{EP}(Q_{REF}(t))| \quad (5)$$

Where,  $\tau_{peak}$  of  $Q_{DRM}(t)$  is the time instant of the maximum amplitude and  $\tau_{base}$  of  $Q_{DRM}(t)$  is taken as the time duration from  $t=0$  ms to the time taken to decay 99% of the peak amplitude of  $Q_{DRM}(t)$  as illustrated in fig. 2. The  $\tau_{peak}$  of  $Q_{REF}(t)$  and  $\tau_{EP}$  of  $Q_{REF}(t)$  is indirectly obtained from  $P(t)$ . The  $\tau_{EP}$  of  $Q_{REF}(t)$  is defined as the time duration between the opening and closing of the aortic valve for each cardiac cycle. The opening of the aortic valve corresponds to the time instant of the systolic foot ( $\tau_{SF}$ ), and the closure of the aortic valve corresponds to time instant of dicrotic notch ( $\tau_{DN}$ ) in the  $P(t)$ . Therefore,  $\tau_{EP}$  is approximated as,

$$\tau_{EP}(Q_{REF}(t)) \cong |\tau_{DN}(P(t)) - \tau_{SF}(P(t))| \quad (6)$$

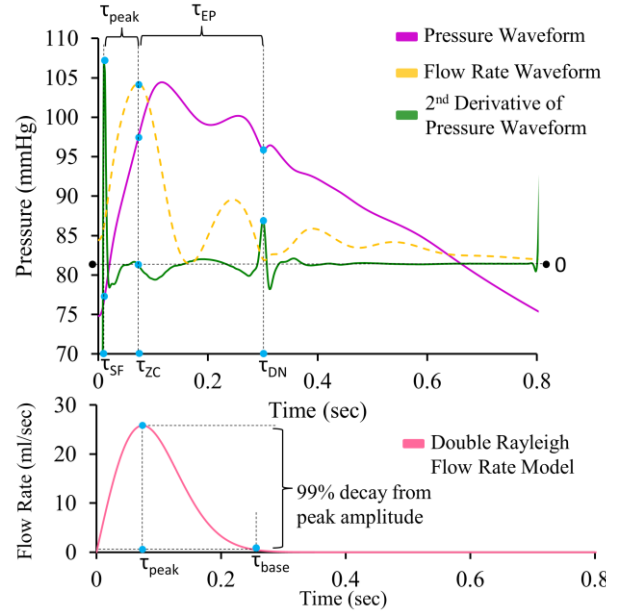


Fig.2. Construction of double-Rayleigh flow rate model

The  $\tau_{peak}$  of  $Q_{REF}(t)$  is approximated from the second derivative zero-crossing ( $\tau_{ZC}$ ) or maxima/inflection point ( $\tau_{IP}$ ) before the systolic peak waveform of the transmural pressure [6] as,

$$\tau_{peak}(Q_{REF}(t)) \cong |\tau_{ZC}(P(t)) - \tau_{SF}(P(t))| \quad (7)$$

### B. Data Preparation and Processing

The validation of the developed methods was performed on 4374 virtual (healthy) participants aged from 25 to 75 years. This virtual subject's database was developed by the Hemodynamic research group, Kings College, London, UK [12] based on 1D numerical modelling of the arterial vasculature. The database was created for each age decade (25 years to 75 years), based on the age-related variability in the cardiac, arterial, vascular bed and blood properties. Pressure waveform (in mmHg) and flow rate waveform (in ml/s) obtained for the common carotid artery were utilized in this study.

All the waveforms were sampled at 500 Hz. To derive the fiducial points necessary for implementing the double-Rayleigh flow rate model, the second derivative of the pressure waveform cycle was obtained after pre-processing with a zero-

phase 2<sup>nd</sup> order Butterworth filter of cut-off frequency 75 Hz. The  $\tau_{\text{peak}}$  was computed from the positive to negative zero-crossing of the second derivative waveform after the systolic foot maxima [6]. In some cases, the inflection point (the second derivative maxima before the systolic peak) were also used for computing  $\tau_{\text{peak}}$ . The dicrotic notch was identified as a local maximum in the second derivative waveforms after the occurrence of a systolic peak. The model parameters of  $Q_{\text{DRM}}(t)$  were obtained optimally and the peak amplitude was normalized to 1. To perform WSA, the  $Z_C$  was obtained from the input impedance analysis ( $P(j\omega)/Q_{\text{REF}}(j\omega)$ ) and ( $P(j\omega)/Q_{\text{DRM}}(j\omega)$ ) in the frequency domain. The  $Z_C$  was estimated as the average magnitude of the input impedance from 4<sup>th</sup> to 10<sup>th</sup> harmonics of input impedance [7], [9].

### C. Statistical Analysis

The group average data are presented as mean  $\pm$  standard deviations. All errors are reported as root-mean-square errors (RMSE). Comparison among methods is performed using regression analysis and Bland-Altman analysis. The correlation was reported in terms of Pearson's correlation coefficient ( $r$ ) and statistical significance in the  $p$ -value. Box-and-whisker plots and t-test paired two sample for means were used to indicate the similarity or difference between estimated quantities across the population. The level of significance of  $\alpha = 0.05$  was used for all tests. A  $p$ -value  $< 0.05$  confirmed a statistical significance to reject the associated null hypothesis.

## III. RESULTS AND DISCUSSIONS

### A. Reliability of Double Rayleigh Flow Rate Model

Fig. 3 illustrates a comparison between the  $Q_{\text{DRM}}(t)$  and  $Q_{\text{REF}}(t)$ . The mean time instants of the peak flow rate between  $Q_{\text{DRM}}(t)$  and  $Q_{\text{REF}}(t)$  were  $60 \pm 10$  ms and  $58 \pm 12$  ms respectively and their differences in magnitude were negligible ( $p > 0.05$ ). The mean ejection period of  $Q_{\text{DRM}}(t)$ , was  $276 \pm 40$  ms, whereas the mean value of the ejection period of  $Q_{\text{REF}}(t)$ , (as calculated from dicrotic notch of  $P(t)$ ) was  $300 \pm 24$  ms. The ranges of ejection period (270 ms to 300 ms) reported in literature [9], in coherence with the values obtained in this analysis.

### B. Quantification of Reflection from WSA

An RMSE of  $1.39 \pm 0.99$  mmHg and  $1.45 \pm 0.94$  mmHg was obtained for forward and backward pressure waveforms obtained from  $\text{DRM}_{\text{WSA}}$  upon comparing with  $\text{REF}_{\text{WSA}}$ . The group average for  $\Delta P_F$ ,  $\Delta P_B$  obtained from  $\text{DRM}_{\text{WSA}}$  were  $22.90 \pm 6.78$  mmHg and  $18.34 \pm 7.24$  mmHg respectively and for RM, RI and RWTT were  $0.78 \pm 0.14$ ,  $43.71 \pm 4.83$  % and  $58 \pm 10$  ms respectively. The group average for  $\Delta P_F$ ,  $\Delta P_B$  obtained from  $\text{REF}_{\text{WSA}}$  were  $22.69 \pm 6.78$  mmHg and  $17.85 \pm 6.41$  mmHg respectively and for RM, RI and RWTT were  $0.78 \pm 0.07$ ,  $43.86 \pm 2.42$  % and  $48 \pm 12$  ms respectively. The group average values for  $\Delta P_F$ ,  $\Delta P_B$ , RM and RI among both the methods were comparable ( $p > 0.05$ ) in magnitude.

Similar accuracies of RMSE were reported in the literature for  $P_F(t)$  and  $P_B(t)$  using other simplified WSA techniques in the range of  $0.82 \pm 0.54$  mmHg to  $6.66 \pm 4.67$  mmHg [9]–[11]. Previous studies validating WSA methods for reflection quantification reported similar ranges for  $\Delta P_F$  and  $\Delta P_B$  ( $-0.01 \pm 3.19$  mmHg and  $5.84 \pm 7.18$  mmHg) and RWTT (40 to 100 ms) [13], [14]. The low RMSE of  $P_F(t)$  and  $P_B(t)$  from  $\text{DRM}_{\text{WSA}}$

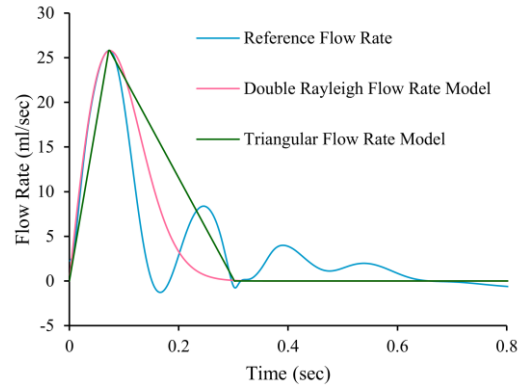


Fig.3. Comparison of double-Rayleigh modelled flow ( $Q_{\text{DRM}}(t)$ ) with actual flow ( $Q_{\text{REF}}(t)$ ) and Triangular flow rate model, scaled to amplitude of the reference peak flow rate for intuitive comparison.

and comparable magnitudes of reflection quantification indices  $\Delta P_F$ ,  $\Delta P_B$ , RM and RI with those obtained from  $\text{REF}_{\text{WSA}}$ , demonstrate the reliability of  $\text{DRM}_{\text{WSA}}$ .

### C. Performance Validation

A statistically significant and strong correlation ( $r > 0.8$ ,  $p < 0.001$ ) was observed for the reflection quantification indices ( $\Delta P_F$ ,  $\Delta P_B$ , RM, RI) obtained from  $\text{DRM}_{\text{WSA}}$  and  $\text{REF}_{\text{WSA}}$ . RWTT obtained from  $\text{DRM}_{\text{WSA}}$  also revealed a statistically significant and moderate correlation ( $r = 0.64$ ,  $p < 0.001$ ) with the counterpart in  $\text{REF}_{\text{WSA}}$ . Bland-Altman analysis for all the reflection quantification indices revealed no clear trend of any systemic progression of errors. The summary of the regression and Bland-Altman analysis is tabulated in TABLE I.

Among the flow-approximated WSA techniques, recent studies have highlighted that triangular flow approximation ( $T_{\text{WSA}}$ ) to carotid flow rate waveform yielded only a moderate correlation for RM and RI ( $r \sim 0.5$ - $0.6$ ) when compared with  $\text{REF}_{\text{WSA}}$  [15]. Studies also suggest  $T_{\text{WSA}}$  is not an appropriate waveform approximation for non-aortic sites [10], [16]. The effect of triangle morphology and the fiducial point identification for implementing  $T_{\text{WSA}}$  was independently studied in [10]. The study concluded that WSA performed using an average flow rate waveform obtained from a small subset of the study population ( $\sim 3\%$ ) performed better than  $T_{\text{WSA}}$ . Further to this, WSA based on Windkessel-modeled flow rate approximation to aortic flow also reported similar accuracies to that of average flow-based WSA [11]. All the above simplified WSA methods are proven to perform better with aortic flow rate approximations and lack evidence in their applicability to non-aortic sites such as carotid flow rate waveforms.

WSA at carotid artery, in the recent past, has reported studies on the mechanism of the pathophysiology of cognitive impairment using wave intensity analysis [17]. The carotid artery has the anatomical advantage of easier access to non-invasive measurement techniques that can simultaneously measure diameter/pressure with flow rate. This has created new avenues in research in studying the effects of acute physiological perturbations such as exercise [18], lower body negative pressure, and cold pressor on carotid artery reactivity, distensibility [19], [20], stiffness/PWV [21] and blood pressure [22]. Being a direct branching of the aorta, the measurements provide a practical solution to study central

TABLE I. PERFORMANCE VALIDATION OF DOUBLE RAYLEIGH FLOW RATE MODEL WSA

Reflection Quantification Indices	Double Rayleigh Flow Rate Model WSA – Reference WSA		
	Regression Analysis	Bland-Altman Analysis	
	Correlation ( <i>p</i> -value)	Bias ( <i>p</i> -value)	Confidence Interval (95%)
Forward Pulse Pressure ( $\Delta P_F$ ) (mmHg)	$r = 0.96$ ( $p < 0.001$ )	0.20 ( $p > 0.05$ )	LC: -3.65; UC: 4.05
Backward Pulse Pressure ( $\Delta P_B$ ) (mmHg)	$r = 0.97$ ( $p < 0.001$ )	0.50 ( $p > 0.05$ )	LC: -3.19; UC: 4.18
Reflection Magnitude (RM)	$r = 0.80$ ( $p < 0.001$ )	0.004 ( $p > 0.05$ )	LC: -0.18; UC: 0.19
Reflection Index (RI) (%)	$r = 0.82$ ( $p < 0.001$ )	-0.15 ( $p > 0.05$ )	LC: -6.31; UC: 6.01
Reflection Wave Transit Time (RWTT) (ms)	$r = 0.64$ ( $p < 0.001$ )	11.12 ( $p < 0.05$ )	LC: -7.38; UC: 29.64

haemodynamics as well. To the best of our knowledge, WSA studies, utilizing non-invasive measurements of pressure and flow rate at the carotid artery were limited [15], [23]–[25]. The DRM<sub>WSA</sub> overcomes certain challenges in our previous work [15] that uses an empirical multi-Gaussian model to perform WSA whose model parameters depended on the study population and requires an initial training with a small subset of the population. In this regard, simplified WSA techniques such as the proposed DRM<sub>WSA</sub>, that minimise the measurements required have the potential to play a vital role in widening the vascular screening procedures and diagnosis by investigating the carotid biomechanics.

#### IV. CONCLUSION

A simplified WSA technique that relies only on a single measurement of pressure waveform was developed. The validation of the method on 4374 healthy virtual subjects, demonstrates the proof of concept. The method could separate the forward-backward components of the pressure waveform and deriving reflection quantification indices such as  $\Delta P_F$ ,  $\Delta P_B$ , RM, RI and RWTT, comparable to the reference WSA methods. This applicability of the proposed DRM<sub>WSA</sub> method to non-aortic sites such as carotid artery has the potential to widen the early vascular screening process, that relies on carotid pulse dynamics.

#### REFERENCES

- [1] J. P. Mynard and A. Kondiboyina, "Wave reflection in the arterial tree," in *Textbook of Arterial Stiffness and Pulsatile Hemodynamics in Health and Disease*, vol. 59, J. A. Chirinos, Ed. Academic Press, 2022, pp. 169–194.
- [2] T. Weber, S. Wassertheurer, M. Rammer, A. Haiden, B. Hametner, and B. Eber, "Wave reflections, assessed with a novel method for pulse wave separation, are associated with end-organ damage and clinical outcomes," *Hypertension*, vol. 60, no. 2, pp. 534–541, 2012.
- [3] A. W. Haider, M. G. Larson, S. S. Franklin, and D. Levy, "Systolic blood pressure, diastolic blood pressure, and pulse pressure as predictors of risk for congestive heart failure in the Framingham Heart Study," *Ann. Intern. Med.*, vol. 138, no. 1, pp. 10–16, Jan. 2003.
- [4] R. Zannoli, P. Schiereck, F. Celletti, A. Branzi, and B. Magnani, "Effects of wave reflection timing on left ventricular mechanics," *J. Biomech.*, vol. 32, no. 3, pp. 249–254, Mar. 1999.
- [5] I. B. Wilkinson et al., "Reproducibility of pulse wave velocity and augmentation index measured by pulse wave analysis," *J. Hypertens.*, vol. 16, no. 12 SUPPL., pp. 2079–2084, Dec. 1998.
- [6] P. Segers et al., "Assessment of pressure wave reflection: Getting the timing right!," *Physiol. Meas.*, vol. 28, no. 9, pp. 1045–1056, 2007.
- [7] N. Westerhof, P. Sipkema, G. C. V. Den Bos, and G. Elzinga, "Forward and backward waves in the arterial system," *Cardiovasc. Res.*, vol. 6, no. 6, pp. 648–656, 1972.
- [8] K. H. Parker, "An introduction to wave intensity analysis," *Med. Biol. Eng. Comput.*, vol. 47, no. 2, pp. 175–188, 2009.
- [9] B. E. Westerhof, I. Guelen, N. Westerhof, J. M. Karemaker, and A. Avolio, "Quantification of wave reflection in the human aorta from

pressure alone: A proof of principle," *Hypertension*, vol. 48, no. 4, pp. 595–601, 2006.

- [10] J. G. Kips et al., "Evaluation of noninvasive methods to assess wave reflection and pulse transit time from the pressure waveform alone," *Hypertension*, vol. 53, no. 2, pp. 142–149, 2009.
- [11] B. Hametner et al., "Wave reflection quantification based on pressure waveforms alone-methods, comparison, and clinical covariates," *Comput. Methods Programs Biomed.*, vol. 109, no. 3, pp. 250–259, 2013.
- [12] P. H. Charlton, J. M. Harana, S. Vennin, Y. Li, P. Chowienczyk, and J. Alastruey, "Modeling arterial pulse waves in healthy aging: a database for in silico evaluation of hemodynamics and pulse wave indexes," *Am. J. Physiol. - Hear. Circ. Physiol.*, vol. 317, no. 5, pp. H1062–H1085, 2019.
- [13] A. Qasem and A. Avolio, "Determination of aortic pulse wave velocity from waveform decomposition of the central aortic pressure pulse," *Hypertension*, vol. 51, no. 2, pp. 188–195, 2008.
- [14] W. Liu et al., "Estimation of aortic pulse wave velocity based on waveform decomposition of central aortic pressure waveform," *Physiol. Meas.*, vol. 42, no. 10, p. 105001, 2021.
- [15] R. Manoj, K. V. Raj, P. M. Nabeel, M. Sivaprakasam, and J. Joseph, "Arterial pressure pulse wave separation analysis using a multi-Gaussian decomposition model," *Physiol. Meas.*, vol. 43, no. 5, p. 055005, May 2022.
- [16] P. Segers et al., "Limitations and pitfalls of non-invasive measurement of arterial pressure wave reflections and pulse wave velocity," *Artery Res.*, vol. 3, no. 2, pp. 79–88, 2009.
- [17] S. T. Chiesa et al., "Carotid artery wave intensity in mid-to late-life predicts cognitive decline: The Whitehall II study," *Eur. Heart J.*, vol. 40, no. 28, pp. 2300–2309, 2019.
- [18] N. Pomella, E. N. Wilhelm, C. Kolyva, J. González-Alonso, M. Rakobowchuk, and A. W. Khir, "Noninvasive assessment of the common carotid artery hemodynamics with increasing exercise work rate using wave intensity analysis," *Am. J. Physiol. - Hear. Circ. Physiol.*, vol. 315, no. 2, pp. H233–H241, 2018.
- [19] J. Joseph, P. M. Nabeel, S. R. Rao, R. Venkatachalam, M. I. Shah, and P. Kaur, "Assessment of Carotid Arterial Stiffness in Community Settings with ARTSENS®," *IEEE J. Transl. Eng. Heal. Med.*, vol. 9, no. November 2020, 2021.
- [20] K. V. Raj, J. Joseph, N. P. M., and M. Sivaprakasam, "Automated measurement of compression-decompression in arterial diameter and wall thickness by image-free ultrasound," *Comput. Methods Programs Biomed.*, vol. 194, p. 105557, 2020.
- [21] R. Arathy, P. M. Nabeel, J. Joseph, and M. Sivaprakasam, "Accelerometric patch probe for cuffless blood pressure evaluation from carotid local pulse wave velocity: Design, development, and in vivo experimental study," *Biomed. Phys. Eng. Express*, vol. 5, no. 4, p. 045010, 2019.
- [22] J. Joseph, P. M. Nabeel, M. I. Shah, and M. Sivaprakasam, "Arterial compliance probe for cuffless evaluation of carotid pulse pressure," *PLoS One*, vol. 13, no. 8, p. e0202480, 2018.
- [23] N. Ohte et al., "Clinical usefulness of carotid arterial wave intensity in assessing left ventricular systolic and early diastolic performance," *Heart Vessels*, vol. 18, no. 3, pp. 107–111, 2003.
- [24] K. Niki et al., "A new noninvasive measurement system for wave intensity: Evaluation of carotid arterial wave intensity and reproducibility," *Heart Vessels*, vol. 17, no. 1, pp. 12–21, 2002.
- [25] N. Pomella, "Non-invasive wave intensity analysis in common carotid artery of healthy humans," no. April, 2017.